Enabling Universal Memory by Overcoming the Contradictory Speed and Stability Nature of Phase-Change Materials

Weijie Wang[1], Desmond Loke[1,2], Luping Shi[1], Rong Zhao[1], Hongxin Yang[1], Leong-Tat Law[1], Lung-Tat Ng[1], Kian-Guan Lim[1], Yee-Chia Yeo[3], Tow-Chong Chong[4] & Andrea L. Lacaita[5]

[1]Data Storage Institute, DSI Building, A*STAR, 5 Engineering Drive 1, Singapore 117608, [2]NUS Graduate School for Integrative Sciences and Engineering, 28 Medical Drive, Centre for Life Sciences #05-01, Singapore 117456, [3]Department of Electrical and Computer Engineering, National University of Singapore, 1 Engineering Drive 3, Singapore 117576, [4]Singapore University of Technology & Design, 20 Dover Drive, Singapore 138682, [5]Dipartimento di Elettronica e Informazione and the IFN-CNR Sez. Milano, Politecnico di Milano, Milano I-20133 Italy.

The quest for universal memory is driving the rapid development of memories with superior all-round capabilities in non-volatility, high speed, high endurance and low power. Phase-change materials are highly promising in this respect. However, their contradictory speed and stability properties present a key challenge towards this ambition. We reveal that as the device size decreases, the phase-change mechanism changes from the material inherent crystallization mechanism (either nucleation- or growth-dominated), to the hetero-crystallization mechanism, which resulted in a significant increase in PCRAM speeds. Reducing the grain size can further increase the speed of phase-change. Such grain size effect on speed becomes increasingly significant at smaller device sizes. Together with the nano-thermal and electrical effects, fast phase-change, good stability and high endurance can be achieved. These findings lead to a feasible solution to achieve a universal memory.

C halcogenides are vital materials used for storing information in phase-change random access memory (PCRAM), which is one of the promising candidates for universal memory. A universal memory can be considered as a single RAM with non-volatility, fast read/write speed, good endurance, high reliability, good CMOS compatibility and low power consumption[1]. PCRAM possesses almost all of the above qualities[2–4]. Its working principle is based on the electrical pulse induced phase-change between the amorphous and crystalline states, and is related to the electric, thermal, mechanical and crystallization properties of phase-change materials. Compared to the amorphization, the crystallization speed is slower and defines the overall writing speed of PCRAMs. There have been tremendous efforts to increase the crystallization speed down to the nanosecond timescale, which have revealed several possible scaling and growth-dominated mechanisms[5–9]. However, the contradictory nature between the crystallization speed and thermal stability of phase-change materials remains the key limitation to achieve fast phase-change[10–12]. The thermal stability has strong dependence on the programming power and endurance of PCRAMs. It is very challenging to realize fast speed and good endurance simultaneously. High speed is achieved at the expense of endurance and stability. This is due to not only the intrinsic material properties, but also the all-round memory requirements. It is well known that when materials reduce to the nanoscale, they show very different properties. They can have a great impact on the phase-change mechanisms, which may allow us to achieve fast speed and high endurance at the same time.
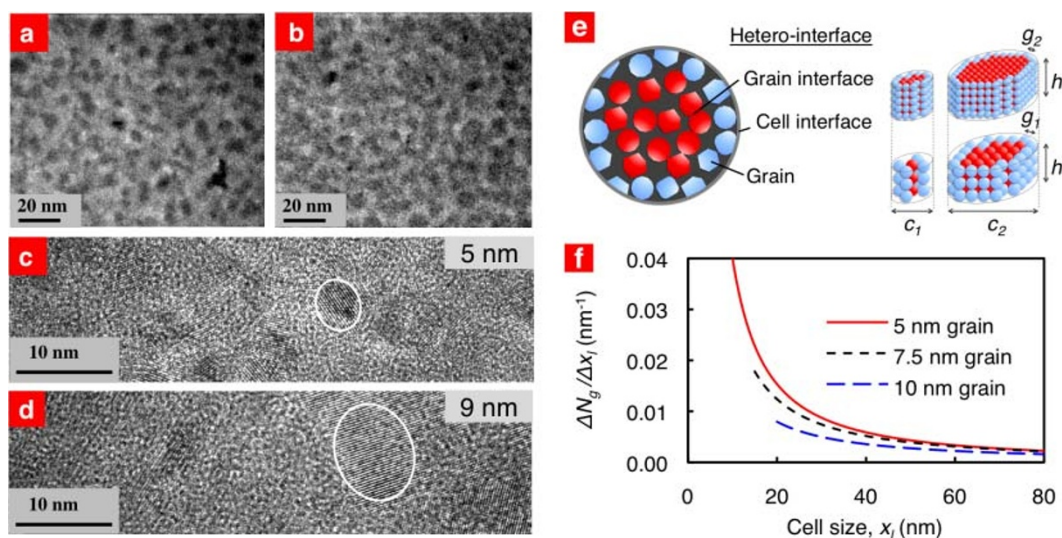
Nitrogen doped $Ge_2Sb_2Te_5$ (NGST) is an intrinsically stable phase-change material and has a higher endurance compared to $Ge_2Sb_2Te_5$ (GST), due to the fact that the excess nitrogen atoms segregate at the grain boundaries[13–15]. However, it has a slower crystallization speed in the hundred-ns, let alone achieve the high writing speed at DRAM levels. In spite of this, NGST has a special feature that enables the control of grain size to achieve very small grain sizes[16–17]. In this study, we discuss a novel approach to achieve both high speed and high endurance via the exploration of the phase-change mechanisms and the grain features of phase-change materials.

Results

Pore-like structured PCRAM cells with different NGST grain and cell sizes were fabricated and their speed performances were investigated. SiO$_2$-on-Si substrate was used as the starting material, on which an electrode comprising of 200 nm thick TiW was formed. A 30 nm thick SiO$_2$ dielectric layer was deposited. It was patterned and etched to form a pore. Pores with diameters ranging from 25 nm to 200 nm were generated and used to define the PCRAM cell sizes. The pore was filled with 40 nm of NGST with 3.5 atomic percent of nitrogen. NGST with grain sizes of 5 nm and 9 nm were employed to study the grain size effect on the switching speed of PCRAMs (see Methods). The different grain sizes were achieved by varying the sputtering power. The grain size was smaller when a lower sputtering power was used. The NGST films were characterized in the amorphous and crystalline phases, as the TEM images show in Figs. 1a) and b), and Figs. 1c) and d), respectively. A 200 nm thick TiW top electrode was deposited and patterned to complete the structure.

In a PCRAM cell, a reduction in the cell size limits the number of grains in a cell and increases the ratio of boundary interfaces. As shown in Fig. 1e), the NGST material in a nanocell has two types of interfaces: a) the cell-interface (CI), which exists between the dissimilar materials, and b) the grain-interface (GI), which separates differently oriented grains of the same material. The CI has a higher ratio of interface-area-to-volume when the cell is smaller. NGST has many grains and grain boundaries; the boundary between the adjacent grains forms the GI. The interplay between the two interfaces CI & GI at the nanoscale can be studied from the perspective of grains in the material-interface system. When the diameter of a cell is reduced, NGST will experience a faster decrease in the number of grains in the inner cores (interior grain), in contrast to the reduction of grains at the CI (exterior grain). We have calculated the change in the effective surface-area-to-volume ratio, which is given by the fraction of exterior grains (ΔN_g) of NGST with respect to the change in cell size (Δx) for different NGST grain sizes (see Methods). From the numerical calculations as shown in Fig. 1f), we can observe that the values of $\Delta N_g/\Delta x$ are small when either or both the grain and cell sizes are large. As both the grain and cell sizes become smaller, the value of $\Delta N_g/\Delta x$ increases sharply. The difference in $\Delta N_g/\Delta x$ for NGST with various grain sizes becomes even larger as the cell size decreases, meaning that the overall interfacial boundary area has increased significantly.

The switching speed of the PCRAM cells with different grain and cell sizes was examined by studying the shortest electrical pulse required for switching the cells from the crystalline state to the amorphous state (reset) and from the amorphous state to the crystalline state (set), as shown in Figs. 2a) and b), respectively. The full-width half-maximum time duration of the pulse was measured just before the PCRAM cell, and this was used to characterize the switching speed of the PCRAM cells (see Methods). The cells were switched reversibly between 10 kΩ and 300 kΩ with constant reset and set voltages of 5 V and 1 V, respectively. Over the entire cell size ranging from 200 nm down to 25 nm, the phase-change speed becomes faster when the cell size reduces. For a given cell size, the cells with grain size of 5 nm has a faster switching speed than that of the cells with grain size of 9 nm. The large cells in the range from 200 nm to 100 nm require pulse-width of a few ns to reset and several tens ns to set. Moving down to the small cells in the range from 100 nm to 25 nm, much shorter pulses were needed for phase-change. The grain size effect on the phase-change speed is different in these two cell size regions. In the region from 200 nm to 100 nm, although the phase-change speed is dependent on the grain size, the speed difference between the 5 nm and 9 nm grain sizes is almost constant and has linear dependence on the cell size. However, in the range from 100 nm to 25 nm, not only the phase-change speed, but also the speed difference between the two grain-sizes increases significantly with cell size reduction. The cells with 5 nm grains require much shorter pulses to switch, as compared to that of the cells with 9 nm grains when the cell size decreases. This is more clearly observed for the set process, which determines the speed of the PCRAM. The speed increment for the grain size from 9 nm to 5 nm at the cell size of 200 nm is only about 3 %. In contrast, the increment at the cell size of 25 nm is as high as 400 %.

Figures 2 c) and d) show the dependence of the switching voltage on the pulse width achieved to reset and set the PCRAM cells with the respective grain and cell sizes of 5 nm and 25 nm. As the pulse width decreases, the minimum voltage required to switch the cell increases. The shortest reset and set pulses achieved were 350 ps and 3 ns, respectively.

The endurance of PCRAM under fast switching condition was studied for a cell with grain and cell sizes of 5 nm and 25 nm, respectively, as shown in Fig. 2e). We have found that the cell can switch reversibly and stably for 10^8 cycles using reset and set pulses as
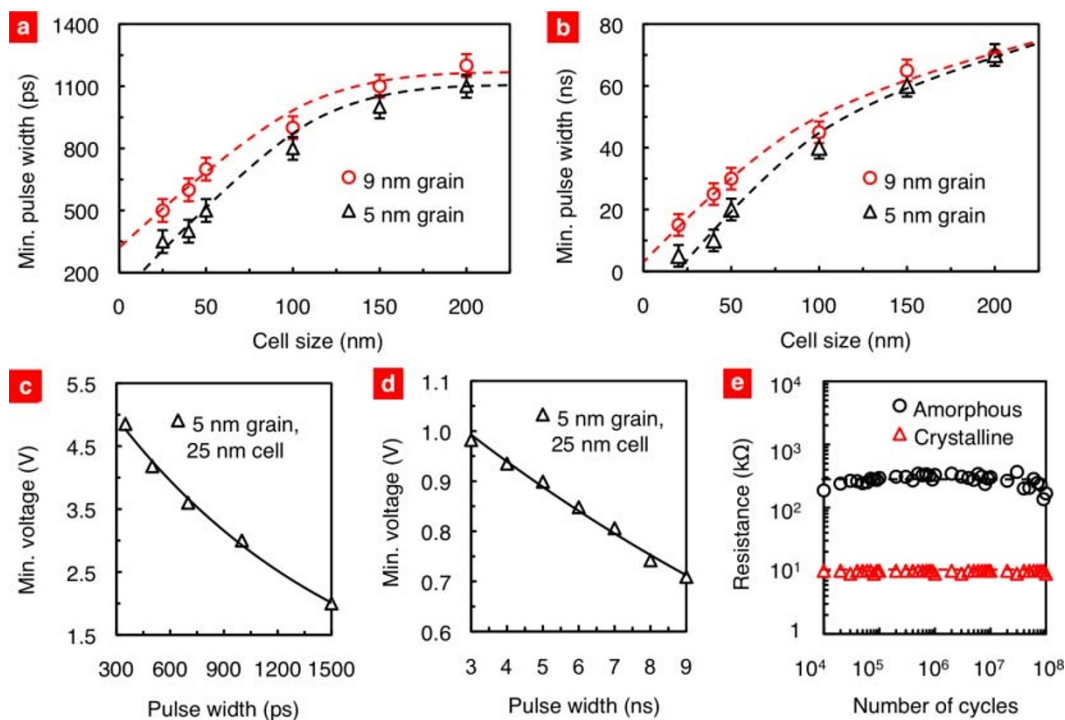

Figure 1 | Interplay between the grain and cell sizes. TEM images of the as-deposited amorphous NGST films obtained with a sputtering power of (a) 0.1 and (b) 0.3 kW, and the annealed crystalline NGST films with grain sizes of (c) 5 and (d) 9 nm. (e) Schematic diagram showing the higher interface-area-to-volume ratio of cells when both the grain and cell size decreases. (f) Numerical study shows that the $\Delta N_g/\Delta x$ increases when both the grain size and cell size reduces. As the cell size falls below 40 nm, the increase in $\Delta N_g/\Delta x$ was observed to be faster for the cells with smaller grain sizes. g_1 and g_2, c_1 and c_2, and h refer to the grain sizes, cell sizes, and material thickness, respectively.

Figure 2 | PCRAM switching performance. Correlation between the minimum pulse-width achieved and cell size for (a) reset and (b) set. As the cell size decreases, the cells with grain size of 5 nm can achieve much shorter pulse-width compared to that of the cells with grain size of 9 nm, by up to 400%. Dependence of the minimum voltage on the pulse-width achieved to (c) reset and (d) set a 25 nm cell. The shortest pulse widths achieved were 350 ps and 3 ns for reset and set, respectively. (e) Cycling endurance of a cell with grain and cell sizes of 5 nm and 25 nm, respectively. Stable and reversible switching for 10^8 cycles was achieved with short reset and set pulse of 6 ns and 9 ns, respectively. This shows that both high speed and high stability can be achieved at the same time.

short as 6 ns and 9 ns, correspondingly. To the best of our knowledge, this is the first time that 10^8 is achieved with both set and reset pulses shorter than 10 ns, which is at the level of DRAM speed. This demonstrates that PCRAM can achieve both fast speed, and high stability at the same time, and such good performance is achieved by reducing both the cell and grain sizes simultaneously.

Discussion

Now, we discuss why higher crystallization speed can be achieved in phase-change materials with intrinsically stable properties, through the scaling of the cell and grain sizes. Considered collectively, the fraction of CI and GI will be larger when the cell size decreases. For a NGST cell with a smaller grain size, the fraction of CI and GI will increase more sharply and result in a much higher effective contact-area-to-volume ratio when their cell sizes are reduced, as being compared to that of a NGST cell with a larger grain size. It is known that imperfections exist at interfaces[18,19]. At both CIs and GIs, there can also exist imperfections such as broken or loosely-bonded atomic structures. The electrons in the atomic structures can be excited and become free electrons when energy is supplied. The free electrons can also be generated via impact ionization[20,21]. In a typical process whereby an electrical pulse is applied to a PCRAM cell, there is a probability of electrons being excited to the higher energy conduction bands. This initiates a series of impact ionization processes, and generates a high concentration of free electrons to switch the material[22,23]. At the same time, a large number of ions will be left in the material. These ions can be distorted from their original equilibrium positions due to the strong repulsive Coulomb force between them[24,25]. The pronounced displacement of ions can induce a permanent structural change[26]. Since materials with both smaller grain and cell sizes have a larger fraction of interface areas, they can generate a higher concentration of free electrons and induce a more pronounced displacement of ions, resulting in a rapid change in the atomic structures[7].

Based on the classical crystallization theory, the crystallization of small dimensional materials can be classified either as nucleation-dominated or growth-dominated according to the contribution of the nucleation and the nuclei growth[27–29]. For a nucleation-dominated material, crystallization occurs mainly via the nucleation of crystallites. For a growth-dominated material, crystallization occurs mainly by the nuclei growth process. It is known that NGST is a nucleation-dominated material. Usually, the heterogeneous nucleation rates are observed to be far higher than the homogeneous nucleation rates[30,31], due to the smaller activation energy at the interface. As shown in the schematic diagrams in Fig. 3 a) and b), in a PCRAM cell, unlike the crystallization of bulk materials, the hetero crystallization, which includes the hetero-nucleation and subsequent growth at the boundary between a phase-change material and another material, and the interfacial-growth at the crystalline (*c*)- and amorphous (*a*)- interface of a phase-change material; occurs in addition to the homogeneous nucleation and nuclei growth:

$$I^{homo\text{-}nucl.} + I^{growth} + H^{interfacial\text{-}growth} + H^{hetero\text{-}nucl.\text{-}growth} \quad (1)$$

where, $I^{homo\text{-}nucl.}$, is the inherent homogenous nucleation, I^{growth}, is the inherent nuclei growth, $H^{interfacial\text{-}growth}$, is the interfacial-growth at the *c*- and *a*- interface of a phase-change material, and $H^{hetero\text{-}nucl.\text{-}growth}$, is the heterogeneous nucleation and subsequent growth at the boundary between a phase-change material and another material, as well as the grain boundaries. With the decrease in the cell and grain sizes, the hetero-crystallization rate (3rd and 4th term in Eq. 1) will increase dramatically, and become the dominant mechanism.

In order to validate it, we have conducted a TEM study. The TEM characterization image in Fig. 3c) reveals the crystallization of a NGST film. We can clearly observe that the crystallization starts
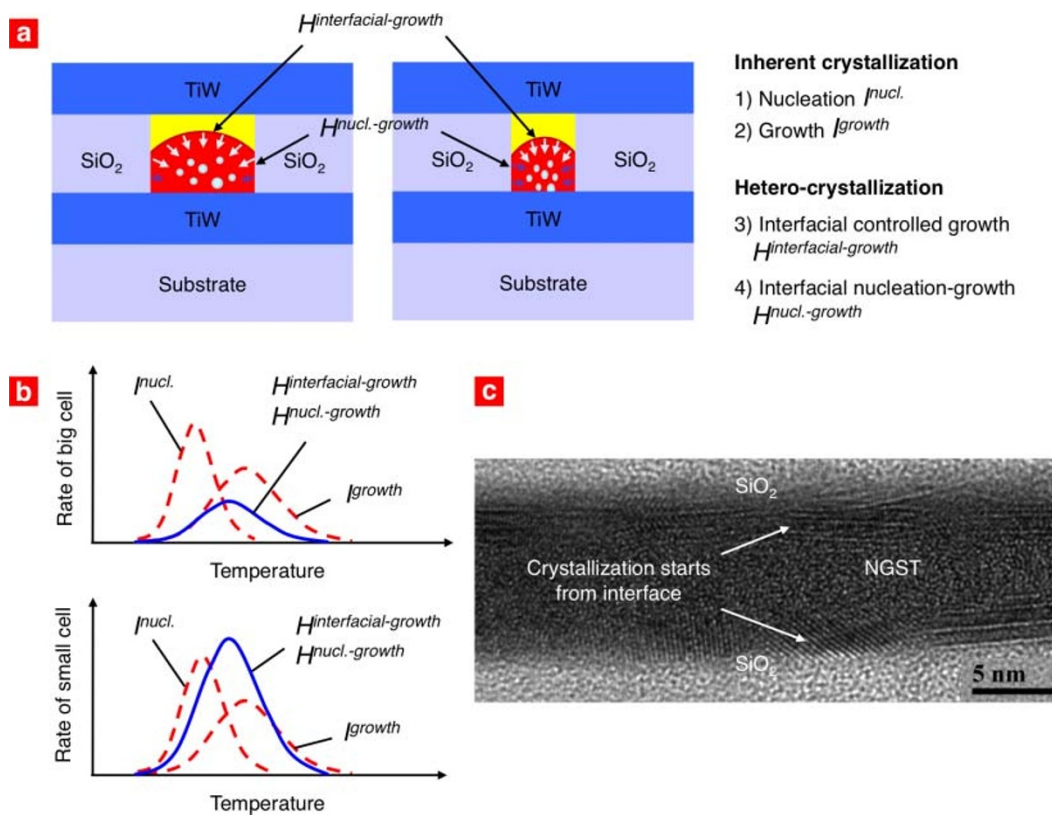
Figure 3 | Dependence of the phase-change mechanism on scaling. (a) Schematic diagram of the phase-change mechanisms in a PCRAM cell that contribute to the phase switching process for different cell sizes. (b) Schematics showing the change in phase-change mechanism. As the cell size decreases, the mechanism changes from the nucleation-dominated to the growth-dominated crystallization process. (c) TEM characterization of the NGST film deposited on SiO$_2$-on Si, and capped with sputtered SiO$_2$. The NGST films were annealed at 280 °C for 3 min. The crystallization starts from the interface, and the grains have different crystalline fringe orientations.

at the interface, and the grains have different crystalline fringe orientations.

On the other hand, as the cell size reduces, the curvature radius of the boundary between the *a*- and *c*-phases becomes smaller. We can apply the periodic bond chain (PBC) theory and attachment energy concept to predict the effect on the crystallization speed[32]. According to the PBC theory, crystallization is dominated by a set of uninterrupted chains of strong bonds formed in the crystal lattice. A smaller curvature radius will increase the statistical number of strong bonds, therefore also facilitating the interfacial-growth $H^{interfacial-growth}$ at the *c*- and *a*- interface (see supplementary information).

The effect of grain size on the phase-change speed can be comprehended by a combinational view of the thermal, crystallization and electrical effects. We have studied the dependence of the resistance on the annealing temperature of the NGST films, as shown in Fig. 4a). A sharper fall in the resistance at higher temperatures is observed for the NGST films with 5 nm grains compared to that of the NGST films with 9 nm grains. This indicates that the smaller grain films have higher "switch-on" temperature, but a faster growth rate. The crystallization behavior of the phase-change materials upon 1- to 3-dimensional scaling has been well studied[6,33–35]. We have studied the effect of scaling on the crystallization process at the device levels. The size dependent crystallization temperature of the PCRAM cells was investigated, as shown in Fig. 4b). The crystallization temperature was determined by observing the onset resistance drop from the reset state to the set state. It can be observed that the crystallization temperature reduces with the cell size, which facilitates fast crystallization. It should be noted that the scaling effect on the crystallization behavior in 2-dimension (just film thickness) is different from that in 3-dimension (phase-change nanoparticles/

nanostructures). In 2-dimension, the crystallization temperature of the phase-change material increases as the thickness decreases[33,34]. In contrast, in 3-dimension, the crystallization temperature of the phase-change material decreases as the diameter decreases[35]. This could be due to the fact that heterogeneous nucleation occurs easily at the non-uniform interface and with difficulty at the flat interface[36].

In the amorphization process, the time needed to form the amorphous area is proportional to the cell size. This effect is studied by simulating (finite element simulation) the size of the heating zone upon pulse activation, as shown in Fig. 4c). A constant pulse is applied and the voltage is kept consistent. We observed that the heating zone becomes smaller as the pulse duration decreases. For complete amorphization to occur, the cell size should be equal/smaller than the heating zone. This means that if a smaller cell is used, it can be completely amorphized with a shorter pulse. This effect is also observed in our experiments. Therefore, by reducing the cell size, the speed of amorphization will also become faster.

It should also be noted that the statistic grain size distribution is expected not to have significant changes during a read/write process. This is mainly due to the fact that the phase-change material in a PCRAM cell can be switched without going through the classical melting process[37,38]. In the related report[37], Kolobov and co-workers have provided an explanation as to why the switching in GST is fast and stable. This is because the crystallization–amorphization process may not necessarily require the rupture of strong covalent bonds. The Te sublattice can be partially preserved as well as the conservation of the local structure around the Sb atoms, and this is a possible reason as to why the transformation is easy and reversible. The material does not have to be transformed into a truly liquid state, and the bond rupture is believed to be due to electronic excitation.

4
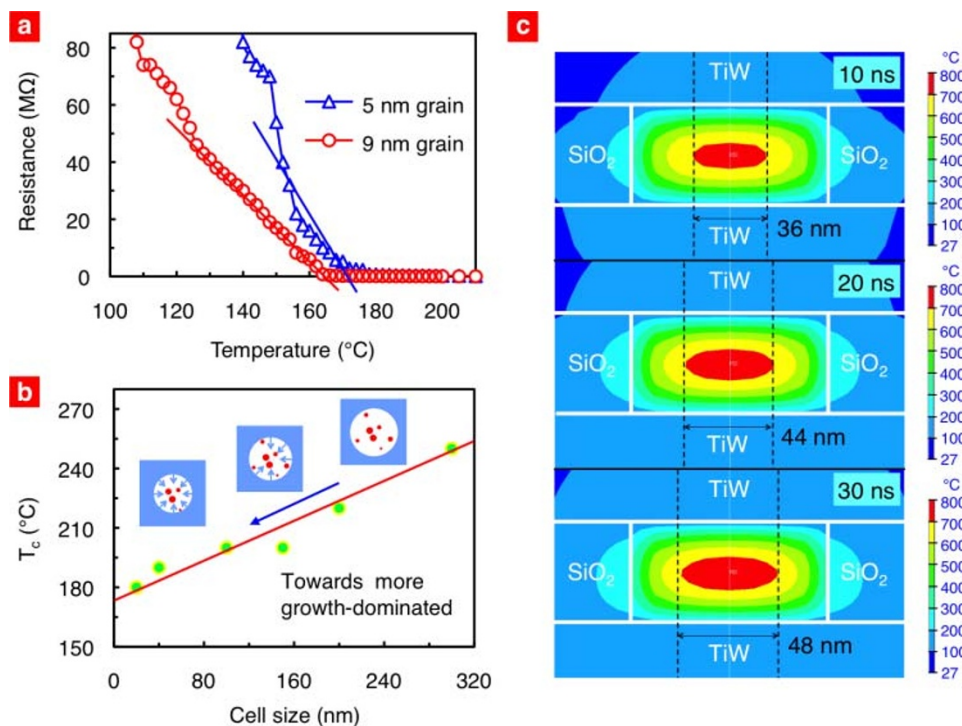
Figure 4 | Nanoeffects of PCRAM. (a) Dependence of the resistance on the annealing temperature of NGST films. Sharper fall in the resistance at higher temperatures is observed for the NGST films with 5 nm grains compared to that of the NGST films with 9 nm grains. (b) Cell size dependent crystallization temperature of PCRAMs. The crystallization temperature becomes lower as the cell size decreases. (c) Simulated temperature profiles of PCRAM in the several 10 ns timescale. Shorter time was needed to phase-change a smaller active region. T_c refers to the crystallization temperature of the phase-change material.

Also, the amorphous structure, at the local level, can be well defined, enhancing the reversibility of the transition. These indicate that the PCRAM can be switched without undergoing the classical melting process. Also, the nitrogen doping effect in phase-change optical media has been well studied and accepted[13]. In NGST, the nitrogen atoms are preferentially bound to Ge in both amorphous and crystalline GST[15,39,40]. As the amount of incorporated nitrogen atoms increases, excess nitrogen atoms in the form of nitrides can segregate at the grain boundaries[15]. These nitrides have been known to inhibit crystal growth, and hence maintain a large number of grain boundaries. During a write process, the GST microcrystal grains melt at around 600 °C. However, the wrapping nitrides remain in the solid phase because the melting temperatures of the nitrides are much higher than that of GST. We have also observed that the grain size is practically unchanged after the PCRAM cell had been switched for 5000 cycles (see supplementary information, Fig. S3). This is the main reason why the overwriting cycle of a phase-change optical disk can be increased from 10^4 to 10^6 by doping nitrogen into GST[13]. The duration of the programming pulses used in this work is within 10 ns, which is much shorter than that used in the optical disk. Thus, we can expect that the grain size distribution in this work to be even better preserved than that in an optical disk. This has been indirectly confirmed by the overwriting of a PCRAM cell for 10^8 cycles.

Based on the results, a possible approach to achieve universal memory is proposed as follows: 1. Select a phase-change material with good stability and endurance. 2. Reduce the cell size to achieve high speed and high endurance at the same time. 3. Further increase the speed by reducing the grain size, which also facilitates the filling of nanoscale pores in the fabrication of PCRAM. 4. In addition, if we can overcome the manufacturing issues to develop an I-shape PCRAM with excellent thermal confinement, even lower operating power is expected.

In conclusion, revealing the transformation of phase-change mechanism with scaling has enabled us to overcome the fundamental limitation that arises from the trade-off between the speed and stability properties of phase-change materials. As the cell size reduces, hetero-crystallization, which includes the interfacial-growth at the phase boundary between the crystalline and amorphous phases, and the heterogenous nucleation and subsequent growth at the boundary between a phase-change material and another material, will become the dominating phase-change mechanism, regardless of the type of phase-change material. Futhermore, higher speed is achieved as the grain size decreases. These findings allow us to utilize phase-change materials with good stability to achieve both fast phase-change speed and good endurance simultaneously. A feasible solution is thus proposed to achieve a universal memory.

Methods

PCRAM fabrication. The PCRAM cells were fabricated using an integrative conventional lithography and nanopatterning techniques. Each patterning step was accomplished using a 365 nm lithography system, followed by a material-deposition and lift-off process. The nanostructures were patterned using an electron beam lithography system (JEOL). All of the materials were deposited using composite targets in a DC magnetron sputtering system (Balzers Cube).

NGST film deposition. The NGST films with 5 and 9 nm grain sizes were deposited using DC magnetron sputtering of a composite GST target and flowing N_2 gas concurrently in a Balzers Cube sputtering system via a reactive sputtering process. The nitrogen concentration in the films was kept consistent by using a constant N_2/Ar gas flow rate of 0.2. The nitrogen and argon flow rates were 3 and 15 SCCM, respectively. The NGST films with grain sizes of 5 and 9 nm were characterized using the X-ray photoelectron spectroscopy (XPS), and the nitrogen concentration in both the films is almost the same at 3.5 at%. The XPS data for the NGST films with 5 and 9 nm grain sizes also showed that their compositions were identical within experimental error. The sputtering power was varied to obtain the NGST films with different grain sizes. The NGST films with 5 nm grain size was obtained when a sputtering power of 0.1 kW was used, while the NGST films with 9 nm grain size was obtained with a sputtering power of 0.3 kW. The grain size was characterized using the Transmission Emission Microscope (TEM) and Atomic force microscope (AFM). The pressure was kept consistent at around 10^{-7} mbar. The thickness of the films was also kept constant at 40 nm.

PCRAM Device Characterization. The PCRAM performance was investigated using an in-house PCRAM testing system. To study the switching speed of the PCRAM cells, electrical pulses with durations and voltages varying from several 100 ps to several 10 ns, and from 0.1 V to 0.4 V, were applied from the pulse generator to the PCRAM cell, respectively. The waveform of the pulse was measured just before the PCRAM cell, and the full-width half-maximum (FWHM) time duration of the waveform was used to characterize the switching speed of the PCRAM cells. The waveform of the pulse collected just after the PCRAM cell also showed that the pulse had passed through the cell, and the FWHM time duration of the pulse is practically unchanged. The PCRAM cell switched from the high resistance state to the low resistance state after the pulse is applied, which means that the pulse had acted on the cell to cause switching. The cells were switched reversibly between the low and high resistance levels of ~ 10 kΩ and ~ 300 kΩ, respectively.

Material study. The material property of NGST was characterized using a TEM (JEOL) and an in-house film resistance measurement system. The TEM was employed to study and calculate the average grain size of the NGST films. The film resistance measurement system was used to measure the film resistance of NGST films during annealing. The annealing temperatures were varied from 100 to 300°C.

Numerical calculation. To study the change in phase-change mechanism, we conducted a numerical study on the change in the effective contact-area-to-volume ratio of phase-change material: the equivalence to the relative change in the fraction of exterior grain (ΔN_g) with respect to the change in material-size (Δx) at different grain and material sizes. To simplify the calculation without affecting the final results, we assumed in the numerical study that the grains of the phase-change material are identical and spherical in shape. They are packed to the maximum number allowable to form cylindrical shapes with varying lateral and vertical material-sizes, both from 10 nm to 90 nm. Various grain-sizes from 5 nm to 10 nm were studied.

1. Marinissen, E. J., Prince, B., Keitel-Schulz, D. & Zorian, Y. Challenges in Embedded Memory Design and Test. *Proceedings of the conference on Design, Automation and Test in Europe* (2005).
2. Ovshinsky, S. R. Reversible electrical switching phenomena in disordered structures. *Phys. Rev. Lett.* **21**, 1450–1453 (1968).
3. Lai, S. & Lowrey, T. OUM - A 180 nm nonvolatile memory cell element technology for stand alone and embedded applications. *IEDM Tech. Digest* 803–806 (2001).
4. Pirovano, A. *et al*. Scaling analysis of phase-change memory technology. *IEDM Tech. Digest* 699–702 (2003).
5. Zhou, G. F. Materials aspects in phase change optical recording. *Material Science and Engineering: A* **304–306**, 73–80 (2001).
6. Lee, S. H., Jung, Y. & Agarwal, R. Highly scalable non-volatile and ultra-low-power phase-change nanowire memory. *Nat. Nanotechnol.* **2**, 626–630 (2007).
7. Wang, W. J. *et al*. Fast phase transitions induced by picosecond electrical pulses on phase change memory cells. *Appl. Phys. Lett.* **93**, 043121-1-3 (2008).
8. Bruns, G. *et al*. Nanosecond switching in GeTe phase change memory cells. *Appl. Phys. Lett.* **95**, 043108-1-3 (2009).
9. Loke, D. *et al*. Ultrafast switching in nanoscale phase-change random access memory with superlattice-like structures. *Nanotechnology* **22**, 254019-1-6 (2011).
10. Yamada, N., Ohno, E., Nishiuchi, K., Akahira, N. & Takao, M. Rapid-phase transitions of GeTe–Sb$_2$Te$_3$ pseudobinary amorphous thin films for an optical disk memory. *J. Appl. Phys.* **69**, 2849–2856 (1991).
11. Wuttig, M. Phase-change materials: Towards a universal memory? *Nat. Mater.* **4**, 265–266 (2005).
12. Kolobov, A. V. Information storage: Around the phase-change cycle. *Nat. Mater.* **7**, 351–353 (2008).
13. Kojima, R. *et al*. Nitrogen doping effect on phase change optical disks. *Jpn. J. Appl. Phys.* **37**, 2098–2103 (1998).
14. Yeh, T. T., Hsieh, T. E. & Shieh, H. P. D. Enhancement of Data Transfer Rate of Phase Change Optical Disk by Doping Nitrogen in Ge–In–Sb–Te Recording Layer. *Jpn. J. Appl. Phys.* **43**, 5316–5320 (2004).
15. Kim, K. *et al*. Observation of molecular nitrogen in N-doped Ge$_2$Sb$_2$Te$_5$. *Appl. Phys. Lett.* **89**, 243520-1-3 (2006).
16. Kim, S. M., Shin, M. J., Choi, D. J., Lee, K. N., Hong, S. K. & Park, Y. J. Electrical properties and crystal structures of nitrogen-doped Ge$_2$Sb$_2$Te$_5$ thin film for phase change memory. *Thin Solid Films* **469–470**, 322–326 (2004).
17. Lai, Y. F. *et al*. Nitrogen-doped Ge$_2$Sb$_2$Te$_5$ films for nonvolatile memory. *J. Electron. Mater.* **34**, 176–181 (2005).
18. Needleman, A. An analysis of decohesion along an imperfect interface. *Int. J. Fract.* **42**, 21–40 (1990).
19. Penn, R. L. & Banfield, J. F. Imperfect Oriented Attachment: Dislocation Generation in Defect-Free Nanocrystals. *Science* **281**, 969–971 (1998).
20. Kim, Y. & Rudd, M. E. Binary-encounter-dipole model for electron-impact ionization *Phys. Rev. A* **50**, 3954–3967 (1994).
21. Sundaram, S. K. & Mazur, E. Inducing and probing non-thermal transitions in semiconductors using femtosecond laser pulses. *Nat. Mat.* **1**, 217–224 (2002).
22. Adler, D., Shur, M. S., Silver, M. & Ovshinsky, S. R. Threshold switching in chalcogenide-glass thin films. *J. Appl. Phys* **51**, 3289–3309 (1980).
23. Pirovano, A. *et al*. Electronic switching effect in phase-change memory cells. *IEDM Tech. Digest* 923–926 (2002).
24. Frasinski, L. J., Codling, K., Hatherly, P., Barr, J., Ross, I. N. & Toner, W. T. Femtosecond dynamics of multielectron dissociative ionization by use of a picosecond laser. *Phys. Rev. Lett.* **58**, 2424–2427 (1987).
25. Dong, Y. & Molian, P. Coulomb explosion-induced formation of highly oriented nanoparticles on thin films of 3C--SiC by the femtosecond pulsed laser. *Appl. Phys. Lett.* **84**, 10–12 (2004).
26. Graves, J. S. & Allen, R. E. Response to GaAs to fast intense laser pulses. *Phys. Rev. B* **58**, 13627–13633 (1998).
27. Coombs, J., Jongelis, A., Es-Spiekman, W. & Jacobs, B. Laser–induced crystallization phenomena in GeTe–based alloys. II. Composition dependence of nucleation and growth. *J. Appl. Phys.* **78**, 4918–4928 (1995).
28. Jeong, T. H., Kim, M. R., Seo, H., Kim, S. J. & Kim, S. Y. Crystallization behavior of sputter-deposited amorphous Ge$_2$Sb$_2$Te$_5$ thin films. *J. Appl. Phys.* **86**, 774–778 (1999).
29. Kalb, J., Spaepen, F. & Wuttig, M. Atomic force microscopy measurements of crystal nucleation and growth rates in thin films of amorphous Te alloys. *Appl. Phys. Lett.* **84**, 5240-1-3 (2004).
30. Christian, J. *Transformation in Metals and Alloys*. 2nd edn. (Pergamon Press, Oxford, 1975).
31. Kelton, K. Crystal nucleation in liquids and glasses. *Solid State Physics* **45**, 75–177 (1991).
32. Hartman, P. & Perdok, W. G. On the relations between structure and morphology of crystals. *I Acta Cryst.* **8**, 49–52, 521 (1955).
33. Raoux, S., Jordan-Sweet, J. L. & Kellock, A. J. Crystallization properties of ultrathin phase change films. *J. Appl. Phys.* **103**, 114310-1-7 (2008).
34. Wei, X. Q., Shi, L. P., Chong, T. C., Zhao, R. & Lee, H. K. Thickness Dependent Nano-Crystallization in Ge$_2$Sb$_2$Te$_5$ Films and Its Effect on Devices. *Jpn. J. Appl. Phys.* **46**, 2211–2224 (2007).
35. Raoux, S., Retter, C. T., Deline, V. R., Philipp, J. B. & Lung, H. L. Scaling properties of phase change nanostructures and thin films. *EPCOS* (2006).
36. Ohshima, N. Crystallization of germanium–antimony–tellurium amorphous thin film sandwiched between various dielectric protective films. *J. Appl. Phys.* **79**, 8357–8363 (1996).
37. Kolobov, A. V. *et al*. Understanding the phase-change mechanism of rewritable optical media. *Nat. Mat.* **3**, 703–708 (2004).
38. Santo, H., Hongo, Y., Tajima, K., Konishi, M. & Saiki, T. Sub-picosecond non-melting structure change in a GeSbTe film induced by femtosecond pulse excitation. *EPCOS* (2009).
39. Kim, Y. *et al*. Change in electrical resistance and thermal stability of nitrogen incorporated Ge$_2$Sb$_2$Te$_5$ films. *Appl. Phys. Lett.* **90**, 021908-1-3 (2007).
40. Caravati, S. *et al*. First-principles study of nitrogen doping in cubic and amorphous Ge$_2$Sb$_2$Te$_5$. *J. Phys.: Condens, Matter* **23**, 265801-1-13 (2011).

Author contribution

W.J.W. and D.L. contributed equally to this work; W.J.W. and D.L. fabricated the PCRAM devices, performed the thermal and electrical characterization and analysis, numerical calculations and simulations, and wrote most of the manuscript; L.P.S. contributed to the project design, leading the project, theoretical modeling, experimental and theoretical analysis, and manuscript writing; R.Z. contributed to the experimental and theoretical analysis, and manuscript writing; H.X.Y. contributed to the fabrication of the nanostructures in the devices; L.T.L. contributed to the characterization of the devices; L.T.N. and K.G.L. contributed to the set-up of electrical characterization system. Y.C.Y., T.C.C., and A.L.L. contributed to the experimental analysis. All authors contributed to the discussion of the manuscript.

Additional information